Catal Lett
DOI 10.1007/s10562-016-1880-9

Silica-Supported Ni(II)–DABCO Complex: An Efficient and Reusable Catalyst for the Heck Reaction

Abdol R. Hajipour[1,2] · **Parisa Abolfathi**[1]

Received: 7 August 2016 / Accepted: 25 September 2016

Abstract An interesting nickel-based catalyst supported on DABCO-functionalized silica was successfully prepared and evaluated as heterogeneous nanocatalyst in Heck cross coupling reaction of various aryl halides and methyl acrylate. The as-prepared nanocatalyst was well characterized by FT-IR, FE-SEM, TEM, XRD, SEM-EDX, ICP and TGA techniques and found to be highly efficient in the reaction system in terms of activity and recyclability.

Graphical Abstract This work provides an economical and heterogeneous catalytic system based nickel nanoparticle supported on DABCO functionalized silica for the Heck cross-coupling reaction of various aryl halides with methyl acrylate.

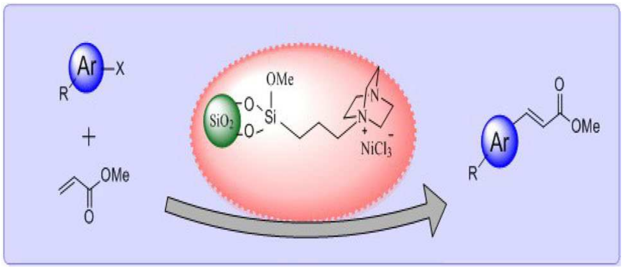

Keywords DABCO · Nickel(II) · Heterogenous catalyst · Mizoroki–Heck reaction

1 Introduction

Metal-catalyzed cross-coupling reactions are one of the most important synthetic methods in organic synthesis [1]. Among the many different protocols for the synthesis of carbon–carbon and carbon–heteroatom bonds, Palladium is the most popular metal used for such reactions in both academic and large-scale synthesis [1, 2]. However, in modern organic synthesis, considerable interest has been focused on palladium-free conditions and development of available and cost-effective transition metal catalysts [3–6]. Cross-coupling of aryl halides and acrylates in Mizoroki–Heck reaction is one of the most efficient routes for the vinylation of aryl halides. Cross-coupling of aryl halides and acrylates in Mizoroki–Heck reaction reaction is one of the most efficient routes for the vinylation of aryl halides, which are an important class of organic compounds and the building blocks of a wide range of biological, pharmaceutical, polymer industries and medicinal chemistry [7–9]. Recently, nickel-based catalytic systems have gained substantial interest in coupling

---

Electronic Supplementary Material The online version of this article (doi:10.1007/s10562-016-1880-9) contains supplementary material, which is available to authorized users.

✉ Abdol R. Hajipour
haji@cc.iut.ac.ir

[1] Pharmaceutical Research Laboratory, Department of Chemistry, Isfahan University of Technology, Isfahan 84156, Iran

[2] Department of Neuroscience, Medical School, University of Wisconsin, 1300 University Avenue, Madison, WI 53706-1532, USA

Scheme 1 The nanocatalyst preparation

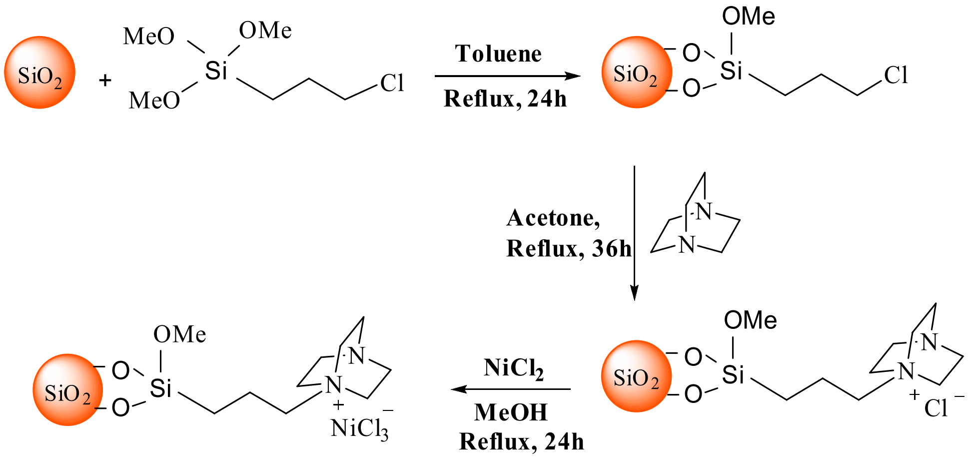

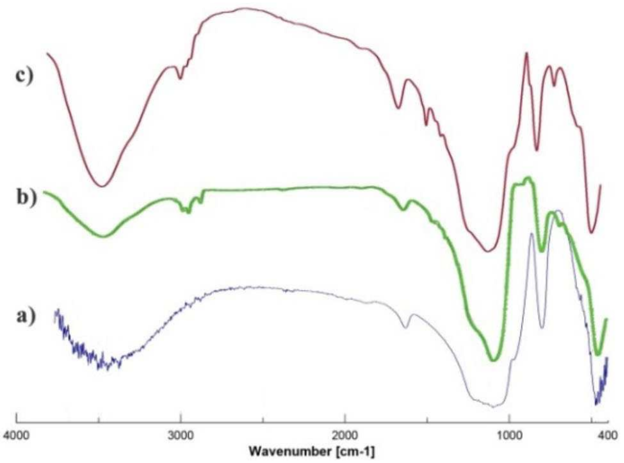

Fig. 1 FT-IR spectra of pure silica (**a**), SiO_2-C_3H_6-Cl (**b**), SiO_2-C_3H_6-DABCO (**c**)

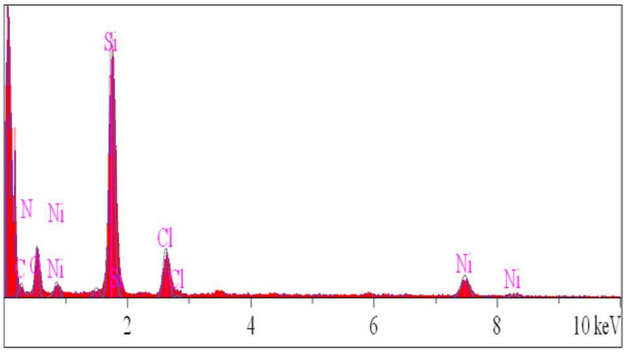

Fig. 2 SEM-EDX spectrum of Ni(II)–DABCO@SiO_2 catalyst

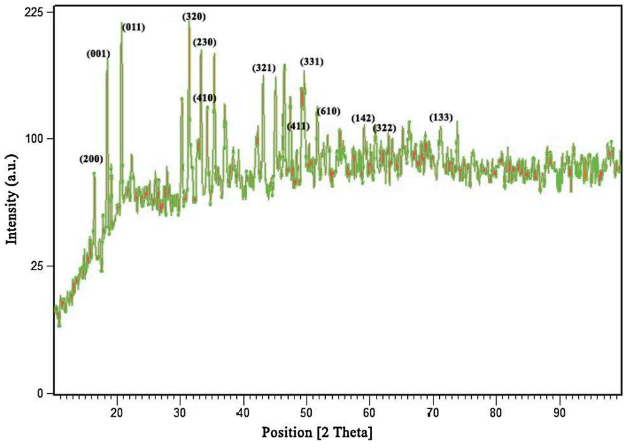

Fig. 3 XRD patterns of Ni(II)–DABCO@SiO_2 catalyst

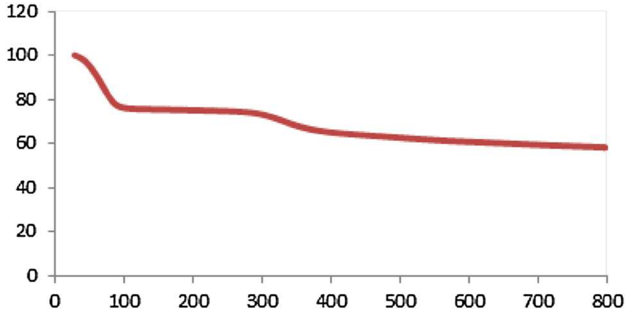

Fig. 4 TGA analysis of Ni(II)–DABCO@SiO_2 catalyst

reactions, in particular, for Heck-type couplings [10–16]. It should be noted that these reactions have been extensively performed in a homogeneous phase, which have some major limitations such as separation and purification of the target product from the reaction media, high toxicity, the lack of recyclability and high catalyst loading (up to 10 mol%) [17–24]. Most of the issues associated with homogenous catalyst can be solved by immobilizing the homogeneous catalysts on various insoluble supports [25–32]. These solid-supported catalysts can be simply separated from reaction mixture via filtration or centrifugation and successfully reused.

Supported catalysts are produced by the reaction of a modified surface with suitable functional groups on the catalyst atoms. There are numerous modification or heterogenization methodologies for metallic species based on various substrates such as silica [33, 34], polymers [35, 36], alumina [37, 38], zeolites [39, 40], carbon nanotube [41–44] and etc. Many different stabilizers such as Ligands [45], polymers [46], ionic liquids (ILs) [47], and dendrimers [48] have been developed as common metal-stabilizers in literature. Grafting of the ionic liquids on the solid-supported catalysts provides a material with a charged surface. It is found that ILs is able to stabilize metallic species through electrostatic interactions. In continuation of our investigations to improve eco-friendly green solid catalyst [35, 49–52], The role of DABCO was investigated by comparing the catalysis with silica supported nickel(II), The DABCO grafted on silica as an effective ligand and a quaternary ammonium salt, plays an important role in increasing the stability and reactivity of metal NPs through the synergistic effect of coordination and electrostatic interactions.

Compared with other ammonium salts, 1,4-Diazabicyclo[2.2.2]octane (DABCO) is known as an inexpensive, eco-friendly, high reactive, easy to handle and non-toxic base catalyst for various organic transformations [53]. The as-prepared material was found to be an efficient and recyclable nanocatalyst for Mizoroki–Heck coupling reaction of various aryl halides with methyl acrylate giving quantitative yields.

2 Experimental

2.1 General Methods

All chemical reagents were purchased from Merck Chemical Company and used without further purification. ^{1}H-NMR spectra were recorded on a Bruker 400 spectrometer using deutrated $CDCl_3$ as solvent and tetramethylsilane (TMS) as internal standard. FT-IR spectroscopy (JASCO FT-IR 680-Plus spectrophotometer) was employed for characterization of products. Also we used Inductive coupled plasma Perkin Elmer Optima 7300 DV. Gas chromatography (GC) (BEIFIN 3420 gas chromatograph equipped with a Varian CP SIL 5CB column: 30 m, 0.32 mm, 0.25 mm) was used for consideration of reaction conversions and yields. Scanning electron micrographs of the catalyst were taken on [FE-SEM, HITACHI (S-4160)]. The 3-*n*-propyl-1-azonia-4-azabicyclo[2.2.2]octane chloride (DABCO-SIL) was prepared according to the literature method [54].

2.2 Preparation of 3-Chloropropyl Functionalized Silica

Silica-gel (1.5 g) was first suspended in hydrochloric acid for 24 h, washed several times with deionized water until the pH value was then adjusted to 7, and dried under vacuum at 120 °C for 8 h. Then, A mixture of dry toluene

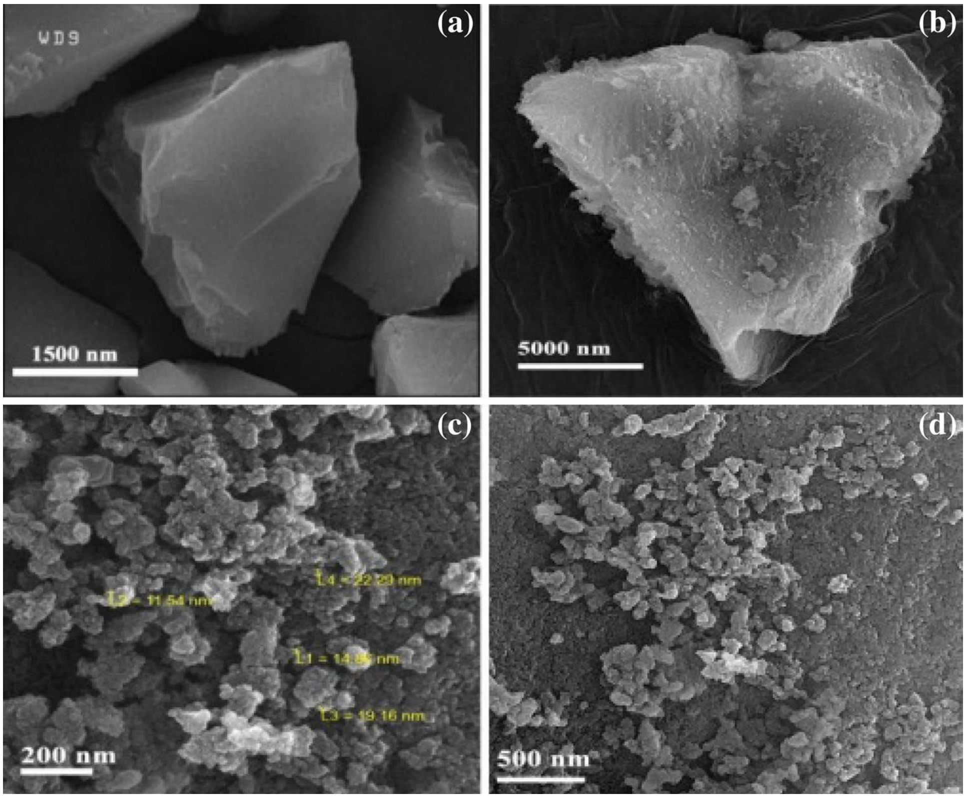

Fig. 5 SEM photographs of Pure SiO_2 (**a**) and Ni(II)–DABCO@SiO_2 (**b**–**d**)

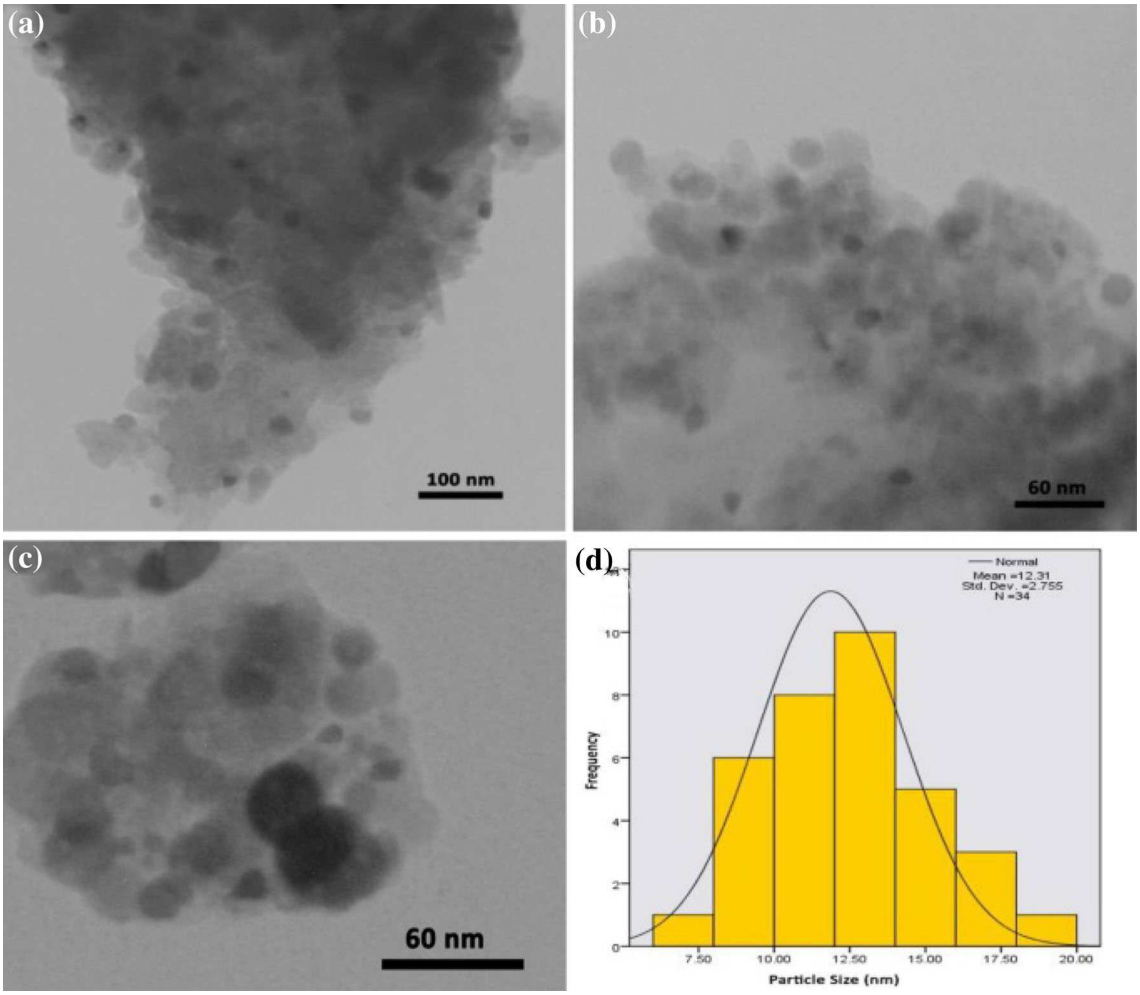

Fig. 6 TEM images of the fresh catalyst (**a, b**) and recovered catalyst (**c**)

(10 mL) and activated silica was refluxed for 24 h after addition of 3-chloropropyltriethoxysilane (1.46 mL) and triethylamine (as a catalyst, 0.2 mL). Afterward, the solvent was decanted and the silica was washed thoroughly with toluene, ethanol, deionized water and methanol. The obtained product was then dried under vacuum drying at 60 °C for 4 h.

2.3 Preparation of Silica Grafted *n*-Propyl-4-aza-1-azoniabicyclo[2.2.2]octane chloride

3-Chloropropyl functionalized silica (1 g) was reacted with 1,4-diazabicyclo[2.2.2]octane (DABCO) (1.12 g, 10 mmol) in dry acetone (40 mL) and refluxed for 36 h to obtain DABCO chloride salt grafted on to the surface of silica (SB-DABCO). Afterward, the reaction mixture was filtered and washed successively with acetone, ethanol, and methanol and dried at 50 °C for 4 h under vacuum.

2.4 Preparation of Ni(II)–DABCO@SiO_2

For preparation of the catalyst, firstly, silica-DABCO (0.5 g) was dispersed in methanol (20 mL). Afterward, $NiCl_2$ (0.25 mmol, 0.032 g) was added to this solution. The mixture was refluxed for 24 h. After stirring, the catalyst was filtered, washed several times with methanol to remove unreacted $NiCl_2$ and dried under vacuum at 50 °C.

3 Results and Discussion

3.1 Preparation and Characterization of the Catalyst

The pathway to synthesize Ni(II)–DABCO@SiO_2 is schematically described in Scheme 1. The compound synthesized was characterized using techniques including elemental analysis (EA), Thermal gravimetric analyses

Table 1 Effect of different parameters for the reaction of bromobenzene with methyl acrylate

Entry	Solvent	T (°C)	Base	Yield[a]
1	DMF	80	K_2CO_3	42
2	DMF	80	K_3PO_4	46
3	DMF	80	KOH	29
4	DMF	80	$NaHCO_3$	38
5	DMF	80	NEt_3	75
6	DMSO	80	NEt_3	70
7	Toluene	80	NEt_3	39
8	EtOH	80	NEt_3	61
9	DMF	90	NEt_3	80
10	DMF	100	NEt_3	95
11	DMF	100	NEt_3	86[b]
12	DMF	100	NEt_3	95[c]

Reaction conditions: bromobenzene (1 mmol), methyl acrylate (1.2 mmol), amount of catalyst (15 mg), time (4 h), base (3 mmol), solvent (4 mL)

[a] Isolated yield

[b] Amount of catalyst used: 10 mg

[c] Amount of catalyst used: 18 mg

(TGA), Inductively coupled plasma analysis (ICP), FT-IR, TEM, SEM, EDX and XRD.

The presence of the functional groups on the silica surface can be observed by FT-IR Spectroscopy. In the FT-IR spectrum depicted in Fig. 1, the absorption peak at 1098 cm^{-1} corresponded to the Si–O–Si vibration. A typical bond around 2924 cm^{-1} should be attributed to aliphatic C–H bond stretching, the signal at 1468 cm^{-1} indicates aliphatic CH_2 bending vibrations and the characteristic peak at 1384 cm^{-1} represents C–N stretching vibration. These facts revealed the successful immobilization of DABCO on the silica surface.

The presence of the organic phase on the silica surface was also confirmed by elemental analysis. Based on the elemental analysis, the loading amount of nitrogen atom was 1.07 mmol g^{-1}. The EDX results indicated the presence of oxygen, nitrogen, silicon, chloride, carbon and nickel in the composites, which confirmed that Ni(II)–DABCO@SiO_2 have been successfully synthesized (Fig. 2). Inductively coupled plasma (ICP) analysis showed that the Ni content was 0.32 mmol g^{-1} in the final solid product. Figure 3 depicts the XRD pattern pattern of catalyst that matched well with that of it (Reference code: 01-079-2297) shows the presence of Ni(II) complex on the amorphous silica support. The wide diffraction peak at $2\theta = 23°$ attributed to SiO_2.

Thermal gravimetric analysis (TGA) was carried out to study the thermal stability of nanocatalyst. TGA of silica/DABCO shows two characteristic decomposition stages (Fig. 4). The mass loss at temperatures below 100 °C was due to the elimination of water molecules from the surface of the silica material and the second mass loss above 300 °C was attributed to the decomposition of the organic groups grafted to the silica surface. Thus, the TGA analysis results demonstrate that the catalyst is stable over 300 °C.

Size, shape and morphology of the nanocatalyst were investigated using Scanning electron microscopy (FE-SEM) and transmission electron microscopy (TEM) imaging techniques (Fig. 5). As displayed in Fig. 6, TEM images of the fresh catalyst confirm that nickel nanoparticles were created in discrete spherical shape without any signs of aggregations. The particle size histogram depicts that nanosized particles have average diameter ranging about 13 nm (Fig. 6d), indicating that DABCO-SiO_2 support can effectively isolate adjacent Ni nanoparticles.The micrograph obtained by SEM showed a clear change in morphology after immobilization of organic groups on to the silica support (Fig. 5b). As shown in Fig. 5c, d, the organic components with spherical morphology and nanometer-sized particles were created on the surface of silica.

3.2 Catalytic Tests

To evaluate the catalytic activity of the nanocatalyst and to determine optimal conditions for Mizoroki–Heck cross-coupling reaction, methyl acrylate and bromobenzene was selected as model substrates and were examined under different parameters such as bases, solvent, temperature conditions and catalyst loading (Table 1). In our first set of experiments, the model reaction was performed in the presence of DMF as a solvent and 15 mg of catalyst in different bases at 80 °C. The results revealed that the yield of product was enhanced to 75 % when NEt_3 was used as base. Subsequently, we studied the impact of various solvets on the efficiency of this procedure. On the basis of this study, DMF was chosen as the most effective solvent for the reaction. To obtain the optimum temperature, the model reaction was also carry out at different temperatures and it was found that reaction temperature plays a critical role in this catalytic system. As you can see in Table 1, the best result was obtained when the reaction was conducted at 100 °C. We also optimized the catalyst loading, employing different amounts of catalyst. The good reaction time and higher yield were observed when the model reaction was carried out with 15 mg of catalyst. For less than this amount, there was a significant decrease in the percentage yield of the product. After optimization, Ni(II)–DABCO@SiO_2 catalysed Heck reactions were examined with various types of aryl halides (chlorides, bromides and iodides). Results summarized in Table 2 show that aryl iodides and aryl bromides were effectively converted the corresponding Heck

Table 2 Reaction of diverse aryl halides with methyl acrylate

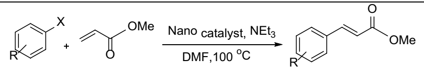

Entry	Ar–X	Product	Time/ h	Yield
1	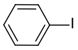	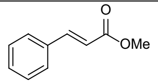	3	97
2	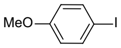	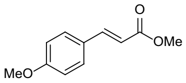	3	94
3	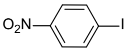	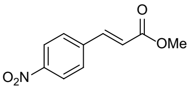	1.5	98
4	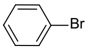	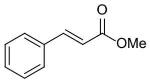	4	95
5	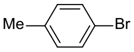	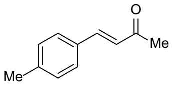	5	87
6	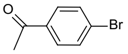	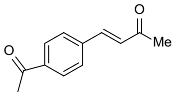	3.5	96
7	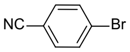	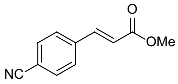	3.5	97
8	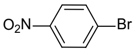	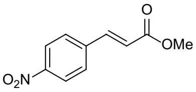	3	97
9	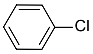	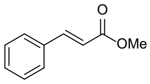	7	84
10	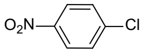	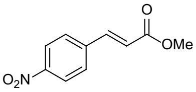	6	87
11	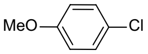	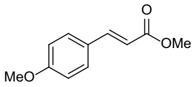	7	79
12	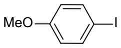	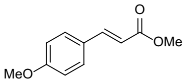	8	72[a]
13	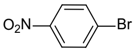	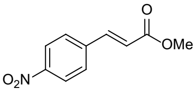	10	67[a]
14	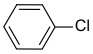	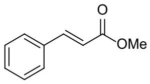	15	31[a]
15	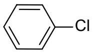	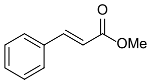	15	47[b]

Reaction conditions: aryl halide (1 mmol), methyl acrylate (1.2 mmol), base (3 mmol), solvent (4 mL), Ni(II)-DABCO@SiO$_2$ catalyst (15 mg), 100 °C, According to isolated yields

[a] Reaction conditions: aryl halide (1 mmol), methyl acrylate (1.2 mmol), base (3 mmol), solvent (4 mL), ligand-Free Ni@SiO$_2$ catalyst (15 mg), 100 °C, Reactions were monitored using GC

[b] Ligand-Free Ni@SiO$_2$ catalyst (25 mg) was used at 120 °C, Reaction was monitored using GCReusability and Heterogeneity Test

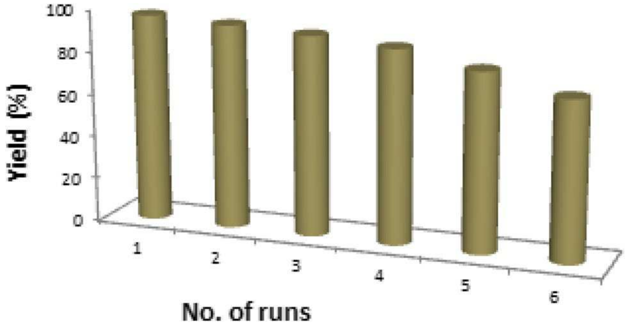

Fig. 7 Reusability of the catalyst in the Suzuki–Miyaura

products in excellent yields. Also, for the less active chlorobenzene and its derivatives a longer time was needed to obtain a moderate yields. The electronic effect on the yields and reaction times was also examined in this reaction system. Overall, the coupling reaction of methyl aclylate with electron withdrawing aryl halides gave better conversions in shorter reaction times. In order to clarify the effect of grafted DABCO on the catalyst performance, a new catalytic system based on nickel immobilized onto silica surface (Ni@SiO$_2$) was easily prepared without the use of DABCO section. This catalytic system was then applied to the Heck coupling of various aryl halides with methyl acrylate (Table 2, entry 12–15). It can be clearly seen that our catalyst is superior to ligand-Free Ni@SiO$_2$ catalyst system in terms of reaction condition, reaction time and yield, indicating that the DABCO as an important functional entity acts as a highly stable linker or/and a chelator to graft catalysts onto silica and increases the stability and reactivity of Ni(II) species during the production process by synergistic effect of coordination and electrostatic interactions.

The level of recyclability of catalyst is highly preferable for its industrial applications. In order to studied this issue, the recovery of the catalyst was examined by using bromobenzene and methyl acrylate under optimized reaction conditions. For this, after each run, the catalytic system was separated from the reaction mixture by filtration and washed with acetone several times, dried at 70 °C, and used for the next cycle. As shown in Fig. 5, this catalyst system could be reusable at least for 6 times without any significant decreasing in its catalytic performance until the fifth reuse. However, the yield of the reaction in the 6th run declined to 74 %. To probe the nature of the active species, i.e., surface or leached Ni, a hot-filtration test was performed by using of bromobenzene and methyl acrylate as coupling partners. The solid catalyst was separated from the reaction mixture after 1 h (34 %, analyzed by GC) and the filtrate was continued for an additional 3 h. After this time, no further improvement in isolated yield was obtained upon catalyst removal. The ICP analysis in good agreement with these results, because only 0.043 ppm of Ni being obtained in the hot filtrate aqueous solution. On the other hand, TEM image of the reused catalyst demonstrates that the structure of Ni/silica has no significant change in comparison with fresh catalyst (Fig. 6c), Also, the observed ICP analysis from the aqueous solution of reaction mixture (after 6th run) displayed only a low amount of nickel metal (0.088 ppm) was leach out from the catalyst, indicating that the attachment between nickel nanoparticles and silica matrix is sufficiently strong (Fig. 7).

4 Conclusions

In conclusion, silica-DABCO-Ni(II) complex nanocatalyst was successfully synthesized and well characterized by different techniques. The obtained product was then used as heterogeneous catalyst for Heck–Mizoroki cross-coupling reaction and exhibited a high catalytic activity and could be easily recovered at least six times.

Acknowledgments We gratefully acknowledge the funding support received for this project from the Isfahan University of Technology (IUT), IR of Iran, and Isfahan Science and Technology Town (ISTT), IR of Iran. Further financial support from the Center of Excellence in Sensor and Green Chemistry Research (IUT) is gratefully acknowledged.

References

1. Diederich F, Stang PJ (2008) John Wiley & Sons, New York
2. Tsuji J (2002) John Wiley & Sons, New York
3. Jana R, Pathak TP, Sigman MS (2011) Chem Rev 111:1417–1492
4. Wang L, Li P, Zhang Y (2004) Chem Commun 5:514–515
5. Yang CT, Zhang ZQ, Liu YC, Liu L (2011) Angew Chem Int Ed 123:3990–3993
6. Zhang L, Zuo Z, Leng X, Huang Z (2014) Angew Chem Int Ed 53:2696
7. Adeli M, Mehdipour E, Bavadi M (2010) J Appl Polym Sci 116:2188–2196
8. Magano J, Dunetz J (2011) Chem Rev 11:2177–2250
9. Nicolaou KC, Bulger PG, Sarlah D (2005) Angew Chem Int Ed 44:4442–4489
10. Bobes FG, Fu GC (2006) J Am Chem Soc 128:5360–5361
11. Leowanawat P, Zhang N, Resmerita AM, Rosen BM, Percec V (2011) J Org Chem 76:9946–9995
12. Knappke CEI, von Wangelin AJ (2010) Angew Chem Int Ed 49:3568–3570
13. Hu X (2011) Chem Sci 2:1867–1886
14. Zultanski SL, Fu GC (2013) J Am Chem Soc 135:624–627
15. Zhang N, Hoffman DJ, Gutsche N, Gupta J, Percec V (2012) J Org Chem 77:5956–5964
16. Xian YL, Guo WH, He GZ, Pan Q, Zhang X (2014) Angew Chem Int Ed 53:1
17. Matsubara R, Gutierrez AC, Jamison TF (2011) J Am Chem Soc 133:19020–19023

18. Tasker SZ, Gutierrez AC, Jamison TF (2014) Angew Chem Int Ed 53:1858–1861
19. Liu C, Tang S, Liu D, Yuan J, Zheng L, Meng L, Lei A (2012) Angew Chem Int Ed 51:3638–3641
20. Rosen BM, Quasdorf KW, Wilson DA, Zhang N, Resmerita AM, Garg NK, Percec V (2010) Chem Rev 111:1346–1416
21. Han FS (2013) Chem Soc Rev 42:5270–5298
22. Zhao YL, Li Y, Li SM, Zhou YG, Sun FY, Gao LX, Han FS (2011) Adv Synth Catal 353:1543–1550
23. Li XJ, Zhang JL, Geng Y, Jin Z (2013) J Org Chem 78:5078–5084
24. Kuroda JI, Inamoto K, Hiroya K (2009) Eur J Org Chem 14:2251–2261
25. Sharma RK, Pandey A, Gulati S (2012) Polyhedron 45:86–93
26. Sharma RK, Pandey A, Gulati S (2012) Appl Catal A 431:33–41
27. Sharma RK, Gulati S (2012) J Mol Catal A Chem 363:291–303
28. Sharma RK, Rawat D (2012) Inorg Chem Commun 17:58–63
29. Sharma RK, Sharma C (2011) Catal Commun 12:327–331
30. Sharma RK, Sharma C (2010) J Mol Catal A Gen 332:53–58
31. Sharma RK, Sharma S (2014) Dalton Trans 43:1292–1304
32. Sharma RK, Sharma S, Gaba G (2014) RSC Adv 4:49198–49211
33. Isfahani AL, Mohammadpoor-Baltork I, Mirkhani V, Khosropour AR, Moghadam M, Tangestaninejad S, Kia R (2013) Adv Synth Catal 355:957–972
34. Singh B, Jain SL, Rana BS, Khatri PK, Sinha AK, Sain B (2010) ChemCatChem 2:1260–1264
35. Hajipour AR, Boostani E, Mohammadsaleh F (2015) RSC Adv 5:24742–24748
36. Kim JH, Kim JW, Shokouhimehr M, Lee YS (2005) J Org Chem 70:6714–6720
37. Nimkar A, Ramana M, Betkar R, Ranade P, Mundhe B (2016) New J Chem 40:2541–2546
38. Kannisto H, Arve K, Pingel T, Hellman A, Harelind H, Eranen K, Olsson E, Skoglundh M, Murzin DY (2013) Catal Sci Tech 3:644–653
39. Kandepi VKM, Narender N (2012) Catal Sci Tech 2:471–487
40. Magne V, Garnier T, Danel M, Pale P, Chassaing S (2015) Org Lett 17:4494–4497
41. Pan HB, Wai CM (2011) New J Chem 35:1649–1660
42. Cornelio B, Rance GA, Laronze-Cochard M, Fontana A, Sapi J, Khlobystov AN (2013) J Mater Chem A 1:8737–8744
43. Rodriguez-Perez L, Pradel C, Serp P, Gomez M, Teuma E (2011) ChemCatChem 3:749–754
44. Sairanen E, Karinen R, Borghei M, Kauppinen EI, Lehtonen J (2012) ChemCatChem 4:2055–2061
45. Amadio E, Scrivanti A, Chessa G, Matteoli U, Beghetto V, Bertoldini M, Rancan M, Dolmella A, Venzo A, Bertani R (2012) J Organomet Chem 716:193–200
46. Ranganath KV, Onitsuka S, Kumar AK, Inanaga J (2013) Catal Sci Tech 3:2161–2181
47. Xu Y, Zhang Z, Zheng J, Du Q, Li Y (2013) Appl Organomet Chem 27:13–18
48. Ornelas C, Ruiz J, Salmon L, Astruc D (2008) Adv Synth Catal 350:837–845
49. Hajipour AR, Azizi G (2013) Green Chem 15: 1030–1034
50. Hajipour AR, Azizi G (2014) RSC Adv 4:20704–20708
51. Hajipour AR, Azizi G (2014) Chin J Catal 35: 1547–1554
52. Hajipour AR, Hosini DM, Mohammadsaleh F (2016) New J Chem. doi:10.1039/c6nj00612d
53. Beheshtia YS, Khorshidi M, Heravi MM, Baghernejad B (2010) Eur J Chem 3:232–235
54. Hasaninejad A, Shekouhy M, Golzar N, Zare A, Doroodmand MM (2011) Appl Catal A Gen 402:11–22